

TWO-STAGE GRID OPTIMIZATION FOR GROUP-WISE QUANTIZATION OF LLMS

Junhan Kim, Gukryeol Lee, Seungwoo Son, Jeewook Kim, and Yongkweon Jeon[†]

Samsung Research

junhankim@islab.snu.ac.kr, {gukryeol.lee, dragwon.jeon}@samsung.com

ABSTRACT

Group-wise quantization is an effective strategy for mitigating accuracy degradation in low-bit quantization of large language models (LLMs). Among existing methods, GPTQ has been widely adopted due to its efficiency; however, it neglects input statistics and inter-group correlations when determining group scales, leading to a mismatch with its goal of minimizing layer-wise reconstruction loss. In this work, we propose a two-stage optimization framework for group scales that explicitly minimizes the layer-wise reconstruction loss. In the first stage, performed prior to GPTQ, we initialize each group scale to minimize the group-wise reconstruction loss, thereby incorporating input statistics. In the second stage, we freeze the integer weights obtained via GPTQ and refine the group scales to minimize the layer-wise reconstruction loss. To this end, we employ the coordinate descent algorithm and derive a closed-form update rule, which enables efficient refinement without costly numerical optimization. Notably, our derivation incorporates the quantization errors from preceding layers to prevent error accumulation. Experimental results demonstrate that our method consistently enhances group-wise quantization, achieving higher accuracy with negligible overhead.

Index Terms— LLM, GPTQ, group-wise quantization, coordinate descent

1. INTRODUCTION

To reduce memory usage and accelerate the inference of large language models (LLMs), quantization has received significant attention recently [1, 2]. Quantization methods can be broadly classified into two classes: quantization-aware training (QAT) [3] and post-training quantization (PTQ) [4]. Although QAT achieves high accuracy by incorporating quantization effects during training, it requires extensive data and expensive retraining. In contrast, PTQ directly quantizes pre-trained models using a small calibration dataset, making it far more practical for billion-scale LLMs [1, 2, 5, 6, 7].

Among PTQ methods, GPTQ has been widely used for its efficiency, quantizing billion-scale LLMs within only a

few hours on a single GPU [1]. In GPTQ, group-wise quantization is often employed to supplement performance in low-bit regimes (e.g., INT2). This strategy partitions each output channel \mathbf{w} into multiple groups $\mathbf{w}_1, \dots, \mathbf{w}_{n_g}$, each of which is assigned a distinct scale s_i (see Fig. 1) to mitigate accuracy loss caused by high intra-channel variance. A key limitation of GPTQ is that it determines scales based solely on the weight perturbation $\|\Delta\mathbf{w}_i\|_2^2$ of an individual group, completely ignoring input statistics \mathbf{X} and inter-group correlations. Consequently, the scales are misaligned with GPTQ’s objective of minimizing the layer-wise reconstruction loss $\|\Delta\mathbf{w}^T \mathbf{X}\|_2^2 = \|\sum_i \Delta\mathbf{w}_i^T \mathbf{X}_i\|_2^2$, leading to suboptimal performance.

In this work, we propose a two-stage optimization framework for group scales that explicitly minimizes the target layer-wise reconstruction loss. In the first stage, conducted prior to GPTQ, we initialize each group scale s_i to minimize the group-wise loss $\|\Delta\mathbf{w}_i^T \mathbf{X}_i\|_2^2$, thereby accounting for input statistics \mathbf{X}_i . In the second stage, we freeze the integer weights obtained via GPTQ and refine the scales to minimize the total layer-wise loss $\|\sum_i \Delta\mathbf{w}_i^T \mathbf{X}_i\|_2^2$. To this end, we employ the coordinate descent algorithm, iteratively updating one scale at a time while keeping the others fixed. We derive a closed-form update rule that enables efficient refinement without the need for costly numerical optimization. Notably, our derivation incorporates the quantization errors from preceding layers to prevent error accumulation across the network. Experimental results demonstrate that our method consistently improves accuracy in group-wise quantization with negligible computational overhead.

2. BACKGROUND

2.1. GPTQ

GPTQ is a PTQ algorithm extensively adopted for the efficient quantization of LLMs [1, 2]. In essence, GPTQ aims to preserve the output of each layer, which is formulated as a layer-wise reconstruction problem:

$$\min_{\mathbf{q} \in \mathcal{Q}} \mathbb{E} \left[\left\| (\mathbf{q} - \mathbf{w})^T \mathbf{X} \right\|_2^2 \right] = \min_{\mathbf{q} \in \mathcal{Q}} (\mathbf{q} - \mathbf{w})^T \mathbf{H} (\mathbf{q} - \mathbf{w}), \quad (1)$$

where \mathbf{q} denotes the quantized weights and $\mathbf{H} = \mathbb{E}[\mathbf{X}\mathbf{X}^T]$ is the Hessian approximation. To solve this, GPTQ first deter-

[†]Corresponding Author

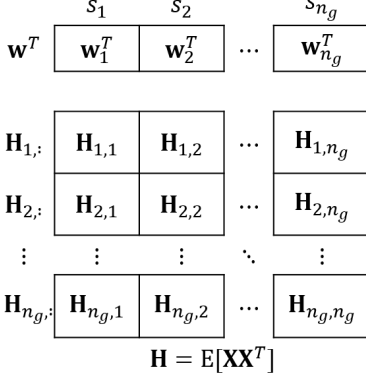


Fig. 1. Illustration of one output channel in a weight matrix and Hessian for group-wise quantization

mines the quantization grid (parameterized by scale factors) and then iteratively performs quantization coupled with error compensation. In each iteration, a single weight is quantized, and the remaining unquantized weights are updated to compensate for the induced error using a Hessian-based update rule [1]. By avoiding time-consuming backpropagation, GPTQ can quantize billion-scale LLMs within a few hours on a single GPU.

2.2. Group-wise Quantization

Typically, channel-wise quantization, which assigns a single scale to each output channel, is favored for its efficiency and broad hardware support. However, at extreme low bit-widths (e.g., INT2), it often incurs severe accuracy degradation because outliers or high intra-channel variance can make scale selection highly susceptible to distribution skew.

Group-wise quantization alleviates this by partitioning \mathbf{w} into multiple groups $\mathbf{w}_1, \dots, \mathbf{w}_{n_g}$ and assigning a separate scale s_i to each group \mathbf{w}_i (see Fig. 1). By allocating distinct scales, the accuracy degradation from high intra-channel variance can be reduced with only a modest increase in dequantization overhead. This strategy is now widely adopted in recent PTQ methods [1, 8] and supported by major LLM inference frameworks such as vLLM [9] and TensorRT-LLM [10].

2.3. Limitation of GPTQ in Group-wise Quantization

Before the iterative process, GPTQ determines the quantization grid by optimizing scales to minimize the layer-wise reconstruction loss in (1), under the assumption that the nearest quantized value is assigned to each weight [11]. For channel-wise quantization, the scale optimization problem is formulated as

$$\begin{aligned} \min_{s>0} \quad & (\mathbf{s}\mathbf{w}_{int} - \mathbf{w})^T \mathbf{H} (\mathbf{s}\mathbf{w}_{int} - \mathbf{w}), \\ \text{s.t.} \quad & \mathbf{w}_{int} = \text{clamp}\left(\left\lceil \frac{\mathbf{w}}{s} \right\rceil, 0, 2^b - 1\right), \end{aligned} \quad (2)$$

where b is the target bit-width. In practice, s is expressed via a clipping factor β with β initialized to one,¹ and the optimal β is determined through a grid search. For group-wise quantization, the presence of multiple scales s_1, \dots, s_{n_g} transforms the objective in (2) into

$$\mathcal{L}(\mathbf{s}) = \sum_{i,j=1}^{n_g} (s_i \mathbf{w}_{int,i} - \mathbf{w}_i)^T \mathbf{H}_{i,j} (s_j \mathbf{w}_{int,j} - \mathbf{w}_j), \quad (3)$$

where $\mathbf{s} = [s_1, \dots, s_{n_g}]^T$, $\mathbf{w}_{int,i}$ denotes the integer weights in the i -th group, and $\mathbf{H}_{i,j} = \mathbb{E}[\mathbf{X}_i \mathbf{X}_j^T]$ represents the cross-correlation between the inputs to groups i and j (see Fig. 1).

Unlike the channel-wise case, a joint grid search over all scales is computationally prohibitive due to its exponential complexity, $\mathcal{O}(M^{n_g})$, where M is the number of candidates for each scale. To simplify this, GPTQ assumes $\mathbf{H} = \mathbf{I}$ (i.e., $\mathbf{H}_{i,i} = \mathbf{I}$ and $\mathbf{H}_{i,j} = \mathbf{0}$ for $i \neq j$), which reduces (3) to a sum of independent group-wise terms $\|s_i \mathbf{w}_{int,i} - \mathbf{w}_i\|_2^2$. While this allows for parallel optimization, it fundamentally ignores input statistics \mathbf{X} and inter-group correlations, leading to suboptimal scale selection. This motivates our method, which explicitly optimizes the scales to minimize the target layer-wise reconstruction loss in (3).

3. PROPOSED METHOD

3.1. Overview: Two-stage Optimization for Group Scales

Our method augments GPTQ with two-stage scale refinement to address its suboptimal grid selection.

Stage 1. Input-aware scale initialization This stage, conducted prior to GPTQ’s iterative process, aims to initialize each group scale s_i by incorporating the corresponding input statistics \mathbf{X}_i . Specifically, we optimize s_i to minimize a local group-wise reconstruction loss $\|\Delta \mathbf{w}_i^T \mathbf{X}_i\|_2^2$, formulated as

$$\begin{aligned} \min_{s_i>0} \quad & (s_i \mathbf{w}_{int,i} - \mathbf{w}_i)^T \mathbf{H}_{i,i} (s_i \mathbf{w}_{int,i} - \mathbf{w}_i), \\ \text{s.t.} \quad & \mathbf{w}_{int,i} = \text{clamp}\left(\left\lceil \frac{\mathbf{w}_i}{s_i} \right\rceil, 0, 2^b - 1\right). \end{aligned} \quad (4)$$

This problem is separable across groups and can therefore be solved efficiently in parallel via independent grid searches. In addition, this step requires no additional memory or computation for $\mathbf{H}_{i,i}$, as it can be directly extracted from the pre-computed Hessian \mathbf{H} (see Fig. 1), which is already available within the standard GPTQ pipeline.

Stage 2. Scale refinement After the iterative process of GPTQ, we *freeze* the integer weights \mathbf{w}_{int} and then refine the group scales \mathbf{s} to minimize the layer-wise reconstruction loss in (3). By doing so, inter-group correlations, which are not considered in the first stage, can be accounted for, while efficiency is maintained because only the scales (rather than

¹ $s = \beta \cdot (\max(\mathbf{w}) - \min(\mathbf{w}))/(2^b - 1)$

the integer weights \mathbf{w}_{int}) are updated. To accomplish this, we employ the *coordinate descent* (CD) algorithm, iteratively updating one scale at a time while keeping the others fixed. Each update step aims to minimize the layer-wise reconstruction loss in (3), thereby yielding scales that are most consistent with the true optimization goal. In the following subsections, we present a closed-form update rule, making the proposed method mathematically grounded and computationally efficient.

3.2. Scale Refinement for the First Layer

Given the assigned integers \mathbf{w}_{int} , we keep them fixed and apply CD to refine the group scales \mathbf{s} . Since the objective is quadratic in each s_i , the optimal s_i^* in each CD step can be obtained by setting $\partial\mathcal{L}/\partial s_i = 0$. Noting that

$$\begin{aligned} \frac{\partial\mathcal{L}}{\partial s_i} &= (2\mathbf{w}_{int,i}^T \mathbf{H}_{i,i} \mathbf{w}_{int,i}) s_i + 2 \sum_{j \neq i} (\mathbf{w}_{int,i}^T \mathbf{H}_{i,j} \mathbf{w}_{int,j}) s_j \\ &\quad - 2 \sum_{j=1}^{n_g} (\mathbf{w}_{int,i}^T \mathbf{H}_{i,j} \mathbf{w}_j), \end{aligned}$$

the closed-form update rule for s_i is derived as

$$\begin{aligned} s_i^* &= \frac{\sum_{j=1}^{n_g} \mathbf{w}_{int,i}^T \mathbf{H}_{i,j} \mathbf{w}_j - \sum_{j \neq i} (\mathbf{w}_{int,i}^T \mathbf{H}_{i,j} \mathbf{w}_{int,j}) s_j}{\mathbf{w}_{int,i}^T \mathbf{H}_{i,i} \mathbf{w}_{int,i}} \\ &= s_i + \frac{\mathbf{w}_{int,i}^T \sum_{j=1}^{n_g} \mathbf{H}_{i,j} (\mathbf{w}_j - s_j \mathbf{w}_{int,j})}{\mathbf{w}_{int,i}^T \mathbf{H}_{i,i} \mathbf{w}_{int,i}}. \end{aligned}$$

Let $\mathbf{H}_{i,:} = [\mathbf{H}_{i,1}, \dots, \mathbf{H}_{i,n_g}]$, and let $\mathbf{q}_j = s_j \mathbf{w}_{int,j}$ be the current quantized weights, then the update rule simplifies to

$$s_i^* = s_i + \frac{\mathbf{w}_{int,i}^T \mathbf{H}_{i,:} (\mathbf{w} - \mathbf{q})}{\mathbf{w}_{int,i}^T \mathbf{H}_{i,i} \mathbf{w}_{int,i}}. \quad (5)$$

Notably, all required terms $\mathbf{H}_{i,i}$ and $\mathbf{H}_{i,:}$ are obtainable directly from the pre-computed Hessian \mathbf{H} (see Fig. 1), requiring no additional memory or computation. For channel-wise quantization where $n_g = 1$, (5) reduces to

$$s^* = s + \frac{\mathbf{w}_{int}^T \mathbf{H} (\mathbf{w} - \mathbf{q})}{\mathbf{w}_{int}^T \mathbf{H} \mathbf{w}_{int}} = \frac{\mathbf{w}_{int}^T \mathbf{H} \mathbf{w}}{\mathbf{w}_{int}^T \mathbf{H} \mathbf{w}_{int}}, \quad (6)$$

which coincides with the result in [12].

3.3. Quantization Error-aware Scale Refinement for Subsequent Layers

In all layers following the first, the input \mathbf{X} differs from the full-precision (FP) input $\tilde{\mathbf{X}}$ due to the quantization of preceding layers. The input deviation $\Delta\mathbf{X} = \mathbf{X} - \tilde{\mathbf{X}}$ can be incorporated into the layer-wise reconstruction error as follows:

$$\begin{aligned} \mathcal{L}(\mathbf{s}) &= \mathbb{E}[\|\mathbf{q}^T \mathbf{X} - \mathbf{w}^T \tilde{\mathbf{X}}\|_2^2] = \mathbb{E}[\|(\mathbf{q} - \mathbf{w})^T \mathbf{X} + \mathbf{w}^T \Delta\mathbf{X}\|_2^2] \\ &= (\mathbf{q} - \mathbf{w})^T \mathbf{H} (\mathbf{q} - \mathbf{w}) + 2\mathbf{w}^T \mathbf{R} (\mathbf{q} - \mathbf{w}) + c, \end{aligned} \quad (7)$$

Algorithm 1 Group-Scale Refinement

Input: FP weights \mathbf{w} , integer weights \mathbf{w}_{int} , number n_g of groups, group size g , initial scales \mathbf{s} , Hessian $\mathbf{H} = \mathbb{E}[\mathbf{XX}^T]$, deviation correlation $\mathbf{R} = \mathbb{E}[\Delta\mathbf{XX}^T]$

Output: Quantized weights \mathbf{q} , optimized scales \mathbf{s}

- 1: Initialize quantized weights: $\mathbf{q} \leftarrow \mathbf{s} \odot_g \mathbf{w}_{int}$
- 2: **for** $i = 0, \dots, n_g - 1$ **do**
- 3: Extract i -th group: $\mathbf{w}_{int,i} \leftarrow \mathbf{w}_{int}[ig : (i+1)g]$
- 4: Extract Hessian blocks:

$$\mathbf{H}_{i,:} \leftarrow \mathbf{H}[ig : (i+1)g, :]$$

$$\mathbf{H}_{i,i} \leftarrow \mathbf{H}[ig : (i+1)g, ig : (i+1)g]$$
- 5: Extract deviation term: $\mathbf{R}_i \leftarrow \mathbf{R}[:, ig : (i+1)g]$
- 6: **Update scale for group i :**

$$s_i \leftarrow s_i + \frac{\mathbf{w}_{int,i}^T \mathbf{H}_{i,:} (\mathbf{w} - \mathbf{q}) - \mathbf{w}^T \mathbf{R}_i \mathbf{w}_{int,i}}{\mathbf{w}_{int,i}^T \mathbf{H}_{i,i} \mathbf{w}_{int,i}}.$$
- 7: Update quantized weights: $\mathbf{q} \leftarrow \mathbf{s} \odot_g \mathbf{w}_{int}$

\odot_g means that each scale s_i multiplies the corresponding group $\mathbf{w}_{int,i}$.

where $\mathbf{R} = \mathbb{E}[\Delta\mathbf{XX}^T]$ and c is a constant with respect to \mathbf{s} . Compared to the loss for the first layer (see (1)), the new loss involves an additional term $\mathbf{w}^T \mathbf{R} (\mathbf{q} - \mathbf{w})$, which explicitly captures the errors introduced by the input deviation $\Delta\mathbf{X}$. Noting that the derivative of this new term is

$$\frac{\partial \mathbf{w}^T \mathbf{R} (\mathbf{q} - \mathbf{w})}{\partial s_i} = \mathbf{w}^T \mathbf{R}_i \mathbf{w}_{int,i}, \quad (8)$$

where $\mathbf{R}_j = \mathbb{E}[\Delta\mathbf{XX}_j^T]$, the update rule for subsequent layers is refined to

$$s_i^* = s_i + \frac{\mathbf{w}_{int,i}^T \mathbf{H}_{i,:} (\mathbf{w} - \mathbf{q}) - \mathbf{w}^T \mathbf{R}_i \mathbf{w}_{int,i}}{\mathbf{w}_{int,i}^T \mathbf{H}_{i,i} \mathbf{w}_{int,i}}. \quad (9)$$

Algorithm 1 summarizes the pseudocode for the proposed CD-based scale refinement stage.

4. EXPERIMENTS

We evaluate our method using the Llama2 and Llama3 models [13]. Following [1], we perform weight-only quantization while keeping activations in FP, which effectively accelerates LLM inference by reducing memory movement. As calibration data, we sampled 128 random sequences of length 2048 from WikiText-2 (Wiki2) [14]. Performance is measured via perplexity (PPL) on the Wiki2 and C4 [15] test splits and average accuracy on several zero-shot commonsense reasoning tasks.² All experiments were conducted on a single NVIDIA H100 GPU (80 GB).

²ARC-challenge and ARC-easy [16], BoolQ [17], OpenbookQA [18], LAMBADA [19], PIQA [20], HellaSwag [21], and WinoGrande [22]

Table 1. Group-wise quantization on Llama (group size=64)

Model	Precision	Method	Wiki2 (↓)	C4 (↓)	0-shot (↑)
Llama3.2-1B -Instruct	FP	baseline	13.16	21.31	56.82
		GPTQ ours	214.7 63.31	429.4 149.5	32.00 33.62
	INT3	GPTQ ours	18.15 16.30	30.73 26.83	50.61 53.19
Llama3.2-3B -Instruct	FP	baseline	11.05	16.49	63.01
		GPTQ ours	73.70 29.33	130.2 80.76	38.55 42.73
	INT3	GPTQ ours	13.43 12.66	19.69 19.58	59.68 61.33
Llama3-8B	FP	baseline	6.139	9.444	70.34
		GPTQ ours	15.07 13.84	209.7 33.14	43.60 49.56
	INT3	GPTQ ours	7.202 7.131	12.53 12.14	66.88 68.74
Llama2-7B	FP16	baseline	5.473	7.266	67.28
		GPTQ ours	13.67 8.274	40.27 13.95	50.35 54.95
	INT3	GPTQ ours	6.171 5.822	8.333 8.097	63.95 65.14
Llama2-13B	FP	baseline	4.885	6.730	69.83
		GPTQ ours	7.248 6.962	12.35 11.88	57.08 59.91
	INT3	GPTQ ours	5.159 5.155	7.320 7.323	68.15 68.65

4.1. Comparison with GPTQ

Tables 1 and 2 summarize the PPL and zero-shot accuracy for GPTQ and the proposed method. The group size, the number of consecutive weights sharing a scale factor, is set to 64 for Table 1 and 32 for Table 2. Overall, performance improves as group size decreases due to the increased number of scale factors. In both cases, the proposed method consistently outperforms GPTQ. For example, under 2-bit quantization, we achieve 6%p and 4%p improvements over GPTQ on Llama3-8B and Llama3.2-3B-Instruct/Llama2-7B, respectively. For small-scale LLMs like Llama3.2-1B-Instruct, the C4 PPL improves significantly ($429.4 \rightarrow 149.5$). Notably, at 3-bit, our method nearly preserves the original FP performance, incurring only a 2%p accuracy drop. This superiority stems from our explicit minimization of the layer-wise reconstruction loss, which accounts for input statistics and inter-group correlations. In contrast, GPTQ determines each group scale independently, thereby ignoring these critical factors.

4.2. Ablation Study

The ablation results in Table 3 highlight the effectiveness of each stage in the proposed scale optimization method. By initializing group scales based on input statistics (stage 1), we achieve substantial PPL improvements on both Wiki2 ($214.7 \rightarrow 130.6$) and C4 ($429.4 \rightarrow 194.0$), with only a minor increase in runtime. The scale refinement stage (stage 2) also

Table 2. Group-wise quantization on Llama3 (group size=32)

Model	Precision	Method	Wiki2 (↓)	C4 (↓)	0-shot (↑)
Llama3.2-1B -Instruct	FP	baseline	13.16	21.31	56.82
		GPTQ ours	113.1 41.11	205.6 87.59	34.14 37.21
	INT3	GPTQ ours	17.40 15.45	28.23 25.33	52.08 53.91
Llama3.2-3B -Instruct	FP	baseline	11.05	16.49	63.01
		GPTQ ours	51.92 22.99	70.63 50.50	41.45 46.57
	INT3	GPTQ ours	14.55 12.29	19.70 18.94	59.34 61.89
Llama3-8B	FP	baseline	6.139	9.444	70.34
		GPTQ ours	13.22 11.52	35.78 24.67	47.09 53.65
	INT3	GPTQ ours	7.417 6.920	12.33 11.59	65.49 69.29

Table 3. Ablation study of each stage on 2-bit group-wise quantization of Llama3.2-1B-Instruct (group size=64)

Method	Stage 1	Stage 2	Wiki2 (↓)	C4 (↓)	Time (min)
GPTQ			214.7	429.4	5.85
ours	✓		130.6	194.0	6.82
		✓	86.15	215.9	6.30
	✓	✓	63.31	149.5	7.53

yields significant gains (Wiki2: $214.7 \rightarrow 86.15$, C4: $429.4 \rightarrow 215.9$) with minimal overhead. Importantly, combining both stages delivers the best performance while maintaining runtime within a reasonable range. These results clearly demonstrate that the two stages are complementary: Stage 1 incorporates input statistics for more reliable initialization, while Stage 2 explicitly accounts for inter-group correlations, jointly enabling the most accurate quantization.

5. CONCLUSION

In this paper, we presented a two-stage optimization framework for group scales to enhance the group-wise quantization performance of GPTQ. In the first stage, group scales are initialized to minimize the group-wise reconstruction loss, effectively incorporating input statistics. In the second stage, conducted after GPTQ’s iterative process, we refine the scales to align with the layer-wise reconstruction objective. To this end, we employed the CD algorithm and derived a closed-form update rule that accounts for quantization errors from preceding layers. Our experimental results demonstrated that the proposed method consistently improves quantization accuracy with negligible computational overhead.

6. REFERENCES

[1] E. Frantar, S. Ashkboos, T. Hoefer, and D. Alistarh, “GPTQ: Accurate post-training quantization for generative pre-trained transformers,” in *International Conference on Learning Representations*, 2023.

[2] S. Ashkboos, A. Mohtashami, M.L. Croci, B. Li, P. Cameron, M. Jaggi, D. Alistarh, T. Hoefer, and J. Hensman, “QuaRot: Outlier-free 4-bit inference in rotated LLMs,” *arXiv:2404.00456*, 2024.

[3] B. Jacob, S. Kligys, B. Chen, M. Zhu, M. Tang, A. Howard, H. Adam, and D. Kalenichenko, “Quantization and training of neural networks for efficient integer-arithmetic-only inference,” in *Proceedings of the IEEE conference on computer vision and pattern recognition*, 2018, pp. 2704–2713.

[4] M. Nagel, R.A. Amjad, M. Van Baalen, C. Louizos, and T. Blankevoort, “Up or down? Adaptive rounding for post-training quantization,” in *International Conference on Machine Learning (ICML)*, 2020, pp. 7197–7206.

[5] J. Kim, C. Lee, E. Cho, K. Park, H. Kim, J. Kim, and Y. Jeon, “Towards next-level post-training quantization of hyper-scale transformers,” in *Advances in Neural Information Processing Systems (NeurIPS)*, 2024, vol. 37, pp. 94292–94326.

[6] J. Kim, H. Kim, E. Cho, C. Lee, J. Kim, and Y. Jeon, “BoA: Attention-aware post-training quantization without backpropagation,” in *Forty-second International Conference on Machine Learning (ICML)*, 2025.

[7] S. Son, W. Park, W. Han, K. Kim, and J. Lee, “Prefixing attention sinks can mitigate activation outliers for large language model quantization,” in *Proceedings of the 2024 Conference on Empirical Methods in Natural Language Processing*, 2024, pp. 2242–2252.

[8] J. Lin, J. Tang, H. Tang, S. Yang, W.M. Chen, W.C. Wang, G. Xiao, X. Dang, C. Gan, and S. Han, “AWQ: Activation-aware weight quantization for on-device LLM compression and acceleration,” in *Proceedings of machine learning and systems*, 2024.

[9] vLLM Team, “vLLM: Easy, fast, and cheap LLM serving,” <https://docs.vllm.ai>, 2025, Accessed: Sept. 2025.

[10] NVIDIA, “TensorRT-LLM: High-performance inference for large language models,” <https://docs.nvidia.com/deeplearning/tensorrt-llm>, 2025, Accessed: Sept. 2025.

[11] Y. Jeon, C. Lee, K. Park, and H. Kim, “A frustratingly easy post-training quantization scheme for LLMs,” in *Proceedings of the 2023 Conference on Empirical Methods in Natural Language Processing*, 2023, pp. 14446–14461.

[12] A. Zhang, Z. Yang, N. Wang, Y. Qi, J. Xin, X. Li, and P. Yin, “COMQ: A backpropagation-free algorithm for post-training quantization,” *arXiv:2403.07134*, 2024.

[13] H. Touvron, L. Martin, K. Stone, P. Albert, A. Almehairi, Y. Babaei, N. Bashlykov, S. Batra, P. Bhargava, S. Bhosale, et al., “Llama 2: Open foundation and fine-tuned chat models,” *arXiv:2307.09288*, 2023.

[14] S. Merity, C. Xiong, J. Bradbury, and R. Socher, “Pointer sentinel mixture models,” *arXiv:1609.07843*, 2016.

[15] C. Raffel, N. Shazeer, A. Roberts, K. Lee, S. Narang, M. Matena, Y. Zhou, W. Li, and P.J. Liu, “Exploring the limits of transfer learning with a unified text-to-text transformer,” *Journal of Machine Learning Research*, vol. 21, no. 1, pp. 5485–5551, 2020.

[16] P. Clark, I. Cowhey, O. Etzioni, T. Khot, A. Sabharwal, C. Schoenick, and O. Tafjord, “Think you have solved question answering? Try ARC, the AI2 reasoning challenge,” *arXiv:1803.05457v1*, 2018.

[17] C. Clark, K. Lee, M.W. Chang, T. Kwiatkowski, M. Collins, and K. Toutanova, “BoolQ: Exploring the surprising difficulty of natural yes/no questions,” *arXiv:1905.10044*, 2019.

[18] T. Mihaylov, P. Clark, T. Khot, and A. Sabharwal, “Can a suit of armor conduct electricity? a new dataset for open book question answering,” *arXiv:1809.02789*, 2018.

[19] D. Paperno, G. Kruszewski, A. Lazaridou, Q.N. Pham, R. Bernardi, S. Pezzelle, M. Baroni, G. Boleda, and R. Fernández, “The LAMBADA dataset: Word prediction requiring a broad discourse context,” *arXiv:1606.06031*, 2016.

[20] Y. Bisk, R. Zellers, J. Gao, Y. Choi, et al., “PIQA: Reasoning about physical commonsense in natural language,” in *Proceedings of the AAAI conference on artificial intelligence*, 2020, vol. 34, pp. 7432–7439.

[21] R. Zellers, A. Holtzman, Y. Bisk, A. Farhadi, and Y. Choi, “HellaSwag: Can a machine really finish your sentence?,” in *Proceedings of the 57th Annual Meeting of the Association for Computational Linguistics*, 2019, pp. 4791–4800.

[22] K. Sakaguchi, R.L. Bras, C. Bhagavatula, and Y. Choi, “WinoGrande: An adversarial winograd schema challenge at scale,” *Communications of the ACM*, vol. 64, no. 9, pp. 99–106, 2021.